



This discussion paper is/has been under review for the journal Atmospheric Measurement Techniques (AMT). Please refer to the corresponding final paper in AMT if available.

A sublimation technique for high-precision measurements of $\delta^{13}\text{CO}_2$ and mixing ratios of CO_2 and N_2O from air trapped in ice cores

J. Schmitt^{1,2}, R. Schneider¹, and H. Fischer^{1,2}

¹Climate and Environmental Physics, Physics Institute, & Oeschger Centre for Climate Change Research, University of Bern, Sidlerstrasse 5, 3012 Bern, Switzerland

²Alfred Wegener Institute for Polar and Marine Research, Bremerhaven, Germany

Received: 17 February 2011 – Accepted: 14 March 2011 – Published: 16 March 2011

Correspondence to: J. Schmitt (schmitt@climate.unibe.ch)

Published by Copernicus Publications on behalf of the European Geosciences Union.

AMTD

4, 1853–1892, 2011

A sublimation
technique for
high-precision
measurements

J. Schmitt et al.

Title Page

Abstract

Introduction

Conclusions

References

Tables

Figures

◀

▶

◀

▶

Back

Close

Full Screen / Esc

Printer-friendly Version

Interactive Discussion



Abstract

In order to provide high precision stable carbon isotope ratios ($\delta^{13}\text{CO}_2$ or $\delta^{13}\text{C}$ on CO_2) from small bubble and clathrate ice core samples we developed a new method based on vacuum sublimation extraction of the CO_2 and gas chromatography-isotope ratio mass spectrometry (GC-IRMS). In a first step the trapped air is quantitatively released from ~30 g of ice and CO_2 together with N_2O are separated from the bulk air components and stored in a miniature glass tube. In an off-line step, the extracted sample is introduced into a helium carrier flow using a minimised tube cracker device. Prior to measurement, N_2O and organic sample contaminants are gas chromatographically separated from CO_2 . Pulses of a $\text{CO}_2/\text{N}_2\text{O}$ mixture are admitted to the tube cracker and follow the path of the sample through the system. This allows an identical treatment and comparison of sample and standard peaks. The ability of the method to reproduce $\delta^{13}\text{C}$ from bubble and clathrate ice is verified on different ice cores. We achieve reproducibilities for bubble ice between 0.05‰ and 0.07‰ and for clathrate ice between 0.05‰ and 0.09‰ (dependent on the ice core used). A comparison of our data with measurements on bubble ice from the same ice core but using a mechanic extraction device shows no significant systematic offset. In addition to $\delta^{13}\text{C}$, the CO_2 and N_2O mixing ratios can be volumetrically derived with a precision of 2 ppmv and 8 ppbv, respectively.

20 1 Introduction

CO_2 concentration measurements on polar ice cores provide direct atmospheric information of past carbon dioxide concentrations over up to the last 800 000 years (Fischer et al., 1999; Petit et al., 1999; Monnin et al., 2001; Lüthi et al., 2008). Refining our quantitative understanding of the observed glacial/interglacial variations in atmospheric CO_2 mixing ratio of about 100 ppmv is an ongoing task of outstanding importance for the paleo climate community (Indermühle et al., 1999; Brovkin et al.,

[Title Page](#)

[Abstract](#)

[Introduction](#)

[Conclusions](#)

[References](#)

[Tables](#)

[Figures](#)

◀

▶

◀

▶

[Back](#)

[Close](#)

[Full Screen / Esc](#)

[Printer-friendly Version](#)

[Interactive Discussion](#)

A sublimation technique for high-precision measurements

J. Schmitt et al.

[Title Page](#)[Abstract](#)[Introduction](#)[Conclusions](#)[References](#)[Tables](#)[Figures](#)[◀](#)[▶](#)[◀](#)[▶](#)[Back](#)[Close](#)[Full Screen / Esc](#)[Printer-friendly Version](#)[Interactive Discussion](#)

by Güllük et al. (1998) was improved by Siegenthaler, their CO₂ data still showed a higher scatter and were less precise than the conventional mechanic crushing method (Siegenthaler, 2002). No attempts to measure $\delta^{13}\text{C}$ using sublimation extraction have been conducted so far.

5 Another issue with respect to $\delta^{13}\text{C}$ measurements regards the limited sample size available from ice cores. In earlier attempts, large sample sizes of up to 1 kg were needed applying the dual inlet technique (Leuenberger et al., 1992; Francey et al., 1999; Smith et al., 1999). This measurement in principle allows for a precision of ~0.05‰ but with the drawback that high sample consumption prevented a high temporal resolution to create a highly resolved record. Furthermore, contamination with drilling fluid caused some erroneous measurements. Here we present a new sublimation extraction-GC-IRMS technique which enables high precision measurement of $\delta^{13}\text{C}$ together with CO₂ and N₂O mixing ratios on 30 g of both bubble and clathrate ice (equivalent to air samples of only 2–3 mL STP (standard temperature and pressure; 15 20 °C and 1 atm)). In contrast to the dual-inlet analysis, sample consumption is considerably reduced by a factor of 10 using the continuous flow inlet technique. In addition, an efficient gas chromatographic sample clean-up is possible removing the drilling fluid contamination and the isobaric component N₂O. Since the gas extraction from the ice is by far more time consuming than the actual IRMS measurement, the system was split 20 into two separate lines. This allows to measure many extracted gas samples within a short time span and, thus, to take benefit of identical measurement conditions in the IRMS for a large set of samples. This is crucial as changes in the performance of the IRMS are a well known problem. Following this technical partition, we first show the setup of the “sublimation extraction” and then the “tube cracker-GC” system connected 25 to the mass spectrometer. Subsequently, the referencing strategy, systematic corrections applied to the data and the performance of the analytical method on air samples and different kind of ice core sample types is discussed. In addition, we compare our data with previous results from other methods to evaluate the absolute accuracy of the measurements.

A sublimation technique for high-precision measurements

J. Schmitt et al.

[Title Page](#)

[Abstract](#)

[Introduction](#)

[Conclusions](#)

[References](#)

[Tables](#)

[Figures](#)

◀

▶

◀

▶

[Back](#)

[Close](#)

[Full Screen / Esc](#)

[Printer-friendly Version](#)

[Interactive Discussion](#)

2 Experimental setup

2.1 General layout

The challenge to measure $\delta^{13}\text{C}$ at high precision together with the CO_2 mixing ratio on small ice samples led to the development of two separate preparation systems (Figs. 1 and 3). With the sublimation extraction (Fig. 1) an ice sample of $\sim 30\text{ g}$ is continuously sublimated. CO_2 , together with N_2O and organic impurities, is cryogenically separated from the major air components (N_2 , O_2 and Ar). After the sublimation of the ice sample is finished, the trapped CO_2 and N_2O fraction is transferred into a small glass tube (Fig. 4). In parallel, the corresponding total air content is determined manometrically. From this, the mixing ratios of CO_2 and N_2O are calculated using the peak area provided by the mass spectrometric measurement. For the GC-IRMS measurement, the tubes are opened within a miniature cracker and the gas sample (CO_2 , N_2O and impurities) is transferred into a He carrier stream (Fig. 3). In a first step, the helium stream is dried, then the sample gases are cryofocused, finally a sharp peak is transferred to a GC column, where the components are separated. The purified CO_2 is admitted to the IRMS via an open split. Both systems are equipped with “reference devices” to either introduce air standards or a $\text{CO}_2/\text{N}_2\text{O}$ mixture in helium, thus, to mimic the ice sample’s way through the various analytic steps.

2.2 Sublimation extraction

2.2.1 General remarks

Degassing of CO_2 from O-rings and polymer based valves and seals, and most notably from glass and metal surfaces from the apparatus itself, are the main sources of contamination, which reduce measurement precision (Güllük et al., 1998; Siegenthaler, 2002; Elsig, 2009). As a consequence, our system was constructed to minimize the total surface of the system and to reduce out-gassing using all-metal seals and valves.

A sublimation technique for high-precision measurements

J. Schmitt et al.

[Title Page](#)

[Abstract](#)

[Introduction](#)

[Conclusions](#)

[References](#)

[Tables](#)

[Figures](#)

◀

▶

◀

▶

[Back](#)

[Close](#)

[Full Screen / Esc](#)

[Printer-friendly Version](#)

[Interactive Discussion](#)



All valves which are in contact with sample CO₂ are all-metal valves (1/4", Fujikin, FUDDFM-71G-6.35, Japan).

The improvements of the original Güllük apparatus by Siegenthaler reduced the total volume of this sublimation line to 1730 mL, whereas our design allowed a further reduction to ~200 mL (for convenience, volume is used as a coarse estimate for surface area). Since their sample size is comparable to ours, we achieved a considerable reduction of the active surface area of the sublimation line exposed to the sample volume. The main improvement was to merge the sublimation vessel and the bulky outer water trap into one vessel. Figures 2 and 3 show the combined sublimation-water trap vessel. This single vessel design required a new cooling strategy using cold air as cooling agent.

2.2.2 Sublimation apparatus

The high vacuum within the sublimation line is provided by a turbo molecular pump backed by a rotary vane vacuum pump (both Leybold Vacuum, Germany). A large, 1/2" diameter water trap (Fig. 1, "water trap 1") held at liquid nitrogen temperature is inserted between the sublimation line and the vacuum pumps to prevent H₂O from entering the high vacuum side. The main advantage of our approach lies in the compact design combining the sublimation of the ice and the close-by removal of the bulk water vapour into one single vessel (33 mm o.d., 121 mm length, CF flange, Caburn, UK) shown in Figs. 1 and 2. This results in two benefits: First, the total surface area is reduced and the number of potentially leaky seals or connections is kept at a minimum. Secondly, it allows fast sublimation rates at low temperatures and, thus, low water vapour pressures due to the high conductance of the large cross section. Consequently, the pressure and temperature difference between the ice sample and the condensed ice in the nearby internal water trap is small due to the high conductivity of the cross section. This is mandatory to achieve a high sublimation rate at low temperature and pressure to keep the ice surface well below -20 °C. Above this temperature, a quasi-liquid layer might

[Title Page](#)

[Abstract](#)

[Introduction](#)

[Conclusions](#)

[References](#)

[Tables](#)

[Figures](#)

◀

▶

◀

▶

[Back](#)

[Close](#)

[Full Screen / Esc](#)

[Printer-friendly Version](#)

[Interactive Discussion](#)

form on the ice surface allowing chemical reactions to take place (Güllük et al., 1998; Barnes et al., 2003).

An air stream of -115°C directed by a cooling jacket allows the upper zone of the sublimation vessel to be cooled to the desired temperature (sublimation is run at around 5 0.25 mbar pH_2O or -34°C). The pressurised air is cooled via a copper heat exchanger mounted in a 2-L Dewar (“cooling device” in Fig. 1). Liquid nitrogen (LN2) is automatically pumped from a reservoir into this heat exchange Dewar until the temperature set-point is reached, with the temperature of the air flow regulated by a thermocouple and a proportional-integral-derivative (PID) controller (West 2300, UK). Although the 10 design of this LN2 pump is basic the resulting temperature of the cooling air can be adjusted fairly constant with changes being $<2^{\circ}\text{C}$ (Schmitt, 2006). The temperature of the cooled air stream can be continuously adjusted from ambient temperature to a lower limit of -150°C , where the system gets unstable due to condensation of O_2 . Via 15 a flow regulator valve and a manometer (V_{air} and P_{air} , Fig. 1) the flow is adjusted to the required demand of coolant from 0 to $\sim 50\text{ L min}^{-1}$, corresponding to a maximum cooling capacity of $\sim 100\text{ W}$ (with a ΔT of $\sim 100^{\circ}\text{C}$ between the cold air stream and the glass vessel). Primarily, the air stream has to remove the latent heat released during the re-sublimation of the water vapour on the wall of the sublimation vessel ($\sim 30\text{ W}$) and secondly to cool the lower part of the glass vessel which absorbs long-wave radiation. 20 Infrared light from halogen bulbs, which surround the sublimation vessel (18 bulbs each with max 30 W at 12 V, Microstar, Osram, Germany) provides the energy for sublimation (Figs. 2 and 3). As the absorption coefficient of ice below 600 nm is small, only the long wave part ($\lambda > 600\text{ nm}$) of the emitted spectrum is used for the sublimation. The emitted light is passed through a special foil filter (Colour Foil, No. 105 orange, LEE, 25 Germany), absorbing the short wave light ($<600\text{ nm}$). Removing the short wave part is a precautionary measure to get rid of the UV part, which could potentially interfere with organic impurities within the ice to produce in-situ CO_2 .

The flange head has two 1/4" feedthroughs, which are connected to the 1/4" tubing (Fig. 1). The left feedthrough is connected to a pressure transducer, “ P_{S} ” (1 Torr max,

[Title Page](#)[Abstract](#)[Introduction](#)[Conclusions](#)[References](#)[Tables](#)[Figures](#)[◀](#)[▶](#)[◀](#)[▶](#)[Back](#)[Close](#)[Full Screen / Esc](#)[Printer-friendly Version](#)[Interactive Discussion](#)

Leybold Vacuum, Germany), to control the H_2O vapour pressure and, thus, temperature during the sublimation. Via valve V2s, the sublimation vessel can be connected to the fore-vacuum to evacuate the sublimation vessel after opening it to load the ice sample. Via valve V2o, the sublimation vessel can be connected to the turbo pump,

5 passing water trap 1 (with $V_{\text{FV}4}$ closed). Onto the right feedthrough, an inlet capillary is mounted which allows the continuous introduction of reference air (see section on air reference inlet). Via valve V3, the sublimation vessel is connected to the external water trap and the consecutive traps.

2.2.3 External water trap

10 Although the internal water trap already removes 99% of the water vapour, an additional, external water trap was needed to achieve the requirements for extreme low pH_2O in the final CO_2 sample. A compact water trap to minimize the total surface area of the system was aimed at. Since in our application the trapped CO_2 and with it any H_2O traces are ultimately transferred into a miniature glass capillary with a volume of 15 μL , a H_2O amount of just 0.1 μg is sufficient to form a liquid phase. In case the H_2O flux exceeds 0.1 μg , liquid H_2O forms within the tube after the transfer from the CO_2 trap to the glass capillary and warming to ambient temperature. The presence of a liquid phase within the tube allows CO_2 to exchange oxygen with H_2O . This shifts the $\delta^{18}\text{O}$ values to more depleted values of up to 5‰. Therefore, temperatures as cold 20 as $-150\text{ }^\circ\text{C}$ in the external water trap are needed to reach the required H_2O vapour pressure and to suppress the formation of a liquid phase in the tube. Since classical cooling systems, e.g. dry ice/pentane slush (Leckrone and Hayes, 1997) are not readily suitable for this temperature range and closed-cycle He coolers are too bulky, we constructed a trap to match our requirements. The trap is made of silitec coated 25 stainless steel tubing (Restec, USA) with 1/4" o.d., 0.53 cm i.d., 20 cm length to reduce adsorption of CO_2 on the cold surface of the trap. This tubing rests within an aluminium block, which is cooled with LN2 droplets and cold nitrogen gas; for details see Schmitt (2006) and Bock et al. (2010). A second reason for the usage of a LN2

cooled water trap is the general exclusion of solvents within our laboratory as traces of organic contaminants are reported to interfere with the IRMS measurement due to isobaric interferences (Francey et al., 1999; Leuenberger et al., 2003; Eyer, 2004). The temperature of the trap is automatically controlled via a thermocouple and a PID controller with an output current driving the “LN2 pump” similar to the air cooling system of the sublimation vessel. Since the trap is operated only 25 °C above the CO₂ saturation pressure during sublimation conditions ($p_{\text{air}} = 0.1$ mbar with $p_{\text{CO}_2} \sim 2.8 \times 10^{-5}$ mbar), cold spots in the trap are of special concern. To detect potential cold spots, we tested the trap by filling it with CO₂ at 0.001 mbar and held the trap at –150 °C for 10 min to observe a pressure drop due to condensation or adsorption. Within the range of precision of the pressure measurement no loss of CO₂ was observed, thus, we are confident that the trap shows no cold spots.

2.2.4 CO₂ trap and glass capillary

From the dried air stream provided by the external water trap, the CO₂ trap removes CO₂, N₂O and organic impurities from the bulk air (O₂, N₂, Ar), which is adsorbed in the consecutive air trap. The CO₂ trap is a 8 cm long, U-formed, 1/8" stainless steel tubing which can be immersed in a dewar filled with LN2 during the trapping procedure (Fig. 3 shows the CO₂ trap in immersed position). After sample collection, the CO₂ trap can be rapidly heated to transfer the gases into the glass capillary. For this, a heating jacket is wrapped around the CO₂ trap to allow heating the trap from –196 °C to +100 °C within 50 s. The tubing and valves enclosed between V4–V5x and V6 (red area in Fig. 1) is permanently heated to 100 °C to minimise CO₂ adsorption during the transfer of the CO₂ to the glass tube.

The tip of an ordinary Pasteur pipet is used to collect and store the extracted CO₂. Prior to usage the glass capillaries are cleaned in an ultrasonic bath with diluted HCl and thoroughly rinsed with deionised water to eliminate organic and inorganic contaminants from the glass surface. The capillary's tip is flame sealed and the diameter of the open end (3 mm o.d.) is adjusted and rounded with a hand torch to fit into the 1/8" o.d.

[Title Page](#)[Abstract](#)[Introduction](#)[Conclusions](#)[References](#)[Tables](#)[Figures](#)[◀](#)[▶](#)[◀](#)[▶](#)[Back](#)[Close](#)[Full Screen / Esc](#)[Printer-friendly Version](#)[Interactive Discussion](#)

Cajon-Ultratorr adapter with which the glass tube is connected with the CO₂ trap via V5. To pump off the atmospheric air from the glass tube and tubing, valve V5x can be connected to the fore-vacuum or after checking the pressure at P_{V5} to the high vacuum (V_{FV4} open, V_{FV3} closed).

5 2.2.5 Air reference inlet

The prerequisite of accurate measurements for isotope analysis is the so called principle of “Identical Treatment” (IT) coined by Werner and Brand (2001). To perfectly fulfil this requirement, one would need artificial ice with air inclusions of known composition. As such a reference material is obviously not available the second best referencing strategy is to continuously admit an air reference during the sublimation of air free ice (“blank ice”). This treatment mimics the air release from the sample during the sublimation as closely as possible. Except for the actual gas release from the ice surface, all subsequent steps are then identical for reference and sample. For referencing we use two pressurised air cylinders with known $\delta^{13}\text{C}$ values and known atmospheric mixing ratios for CO₂ and N₂O. These two air cylinders contain current atmospheric air, with CO₂ mixing ratios being reduced to obtain CO₂ mixing ratios covering the minimum and maximum values during the last 800 ka years. Cylinder CA06195 (“Boulder 1”) has a CO₂ mixing ratio of 182.09 ± 0.04 ppmv, $\delta^{13}\text{C}$ of $-7.92\text{\textperthousand} \pm 0.003\text{\textperthousand}$ with respect to VDPB–CO₂ (the international reference material Vienna Peepee belemnite) and $\delta^{18}\text{O}$ $-4.756\text{\textperthousand} \pm 0.007\text{\textperthousand}$ with respect to VDPB–CO₂. Cylinder CA06818 (“Boulder 2”) has a CO₂ mixing ratio of 296.80 ± 0.02 ppmv, a N₂O mixing ratio of 263.4 ± 3.7 ppbv, $\delta^{13}\text{C}$ of $-8.421\text{\textperthousand} \pm 0.003\text{\textperthousand}$ with respect to VDPB–CO₂ and a $\delta^{18}\text{O}$ $-4.800\text{\textperthousand} \pm 0.014\text{\textperthousand}$ with respect to VDPB–CO₂. The two cylinders were obtained by the Stable Isotope Lab (SIL) at the Institute for Arctic and Alpine Research (INSTAAR), University of Colorado, in cooperation with the Climate Monitoring and Diagnostics Laboratory (CMDL) of the National Oceanic and Atmospheric Administration (NOAA).

[Title Page](#)[Abstract](#)[Introduction](#)[Conclusions](#)[References](#)[Tables](#)[Figures](#)[◀](#)[▶](#)[Back](#)[Close](#)[Full Screen / Esc](#)[Printer-friendly Version](#)[Interactive Discussion](#)

A sublimation technique for high-precision measurements

J. Schmitt et al.

[Title Page](#)[Abstract](#)[Introduction](#)[Conclusions](#)[References](#)[Tables](#)[Figures](#)[◀](#)[▶](#)[◀](#)[▶](#)[Back](#)[Close](#)[Full Screen / Esc](#)[Printer-friendly Version](#)[Interactive Discussion](#)

2.2.6 Volumetric determination of mixing ratios

AMTD

4, 1853–1892, 2011

Although the main purpose of the system lies in the precise determination of $\delta^{13}\text{C}$, it is crucial to measure the mixing ratio of CO_2 and N_2O on the same ice sample with high precision, because: (1) a significant deviation in the CO_2 mixing ratio from neighbouring samples or from different extraction techniques is a valuable tool to detect contamination or loss processes during the whole analysis. (2) For a quantitative interpretation of global atmospheric $\delta^{13}\text{C}$ changes with models, it is imperative to have the data of both the isotopic and the mixing ratio at the same time interval. Although highly resolved time series on CO_2 mixing ratio are available for the Holocene (Monnin et al., 2001; Siegenthaler et al., 2005a), temporal resolution is yet poor and fragmentary during MIS3 and older periods and dating uncertainties as well as a mismatch in the gas age – ice age difference of different cores weaken the precision necessary to entangle global carbon fluxes. (3) Diffusion processes during the transformation of bubble and clathrate ice and below call for extraction techniques which allow 100% extraction efficiencies to provide unfractionated CO_2 concentrations and to validate the measurements on such ice using the classical dry extraction techniques (Lüthi et al., 2010).

With the mass spectrometer providing the amount of CO_2 via the peak area, the amount of the corresponding air is volumetrically determined from the collected gases in the air trap. For this we use a glass tube (1/4" o.d., 1/8" i.d.) filled with 5 Å molecular sieve in pellets (diameter 5 mm, length 20 mm). Before usage and for weekly regeneration, water is removed by heating the molecular sieve to 140 °C for a few hours. During the sublimation, the air trap is immersed into LN2 and acts as a vacuum pump. At –196 °C the equilibrium air pressure above the loaded molecular sieve (2 mL STP air) is <0.0020 mbar ("P_M" pressure transducer, 10⁻⁴ – 1 Torr max). It is therefore the molecular sieve in the air trap that drives the pressure gradient from the sublimation vessel through the external water trap and CO_2 trap to the air trap. The quantitative release of the adsorbed gases is accomplished by heating the trap to +100 °C. The

A sublimation technique for high-precision measurements

J. Schmitt et al.

[Title Page](#)

[Abstract](#)

[Introduction](#)

[Conclusions](#)

[References](#)

[Tables](#)

[Figures](#)

◀

▶

[Back](#)

[Close](#)

[Full Screen / Esc](#)

[Printer-friendly Version](#)

[Interactive Discussion](#)

desorbed air components are expanded into a 2-L expansion volume which is thermally insulated to get a stable temperature reading. After pressure stabilizes within the system, the final pressure and temperature of the expansion volume are read out.

AMTD

4, 1853–1892, 2011

2.3 Tube cracker GC system

5 2.3.1 General remarks

Tube cracker applications are used in many fields of isotope analysis for many decades. Usually, a glass tube containing the extracted gas sample acts as the interface coupling a separate sample preparation step to the isotopic measurement at the dual inlet IRMS. Tube outer diameter dimensions normally used with the latter techniques are 1/4" or 10 even 3/8" and the gas is expanded into the bellow or cold finger of the MS after breaking the tube and before admitting it to the changeover valve. This direct route to the IRMS is not feasible on CO₂ samples from our ice core samples for three reasons. (1) Only small amounts of CO₂ are available since the ice is limited and/or a high temporal resolution and replicates are preferred to get a robust record. (2) Precise $\delta^{13}\text{C}$ values on atmospheric CO₂ samples containing N₂O either involve a mathematic correction for isobaric interference, or the separation of both gases via chromatography (Ferretti et al., 2000). (3) The most important reason for a gas chromatographic separation step prior to the IRMS measurement are organic contaminants from drill fluid, which accompany deep ice core samples and which can interfere in the MS measurement. Since some components of the drill fluid behave physicochemically similar to CO₂ during the extraction process, minute traces of this substance can simultaneously reach the ion source if not separated before. We observed such problems during earlier measurements of drill fluid contaminated ice core samples, which manifested themselves by 20 excessively high m/z 45 and 46 traces yielding highly enriched $\delta^{13}\text{C}$ ratios (>1000‰). Our cryofocus and GC separation avoids these contamination issues. Although a severe contamination can easily be detected by unusual, or physically or climatologically

[Title Page](#)

[Abstract](#)

[Introduction](#)

[Conclusions](#)

[References](#)

[Tables](#)

[Figures](#)

◀

▶

[Back](#)

[Close](#)

[Full Screen / Esc](#)

[Printer-friendly Version](#)

[Interactive Discussion](#)

[Title Page](#)[Abstract](#)[Introduction](#)[Conclusions](#)[References](#)[Tables](#)[Figures](#)[◀](#)[▶](#)[◀](#)[▶](#)[Back](#)[Close](#)[Full Screen / Esc](#)[Printer-friendly Version](#)[Interactive Discussion](#)

unrealistic $\delta^{13}\text{C}$ values and excluded from the data set, minor contaminations are more difficult to detect and require many replicates or a comparison of different cores. In conclusion, gas chromatographic separation of CO_2 from N_2O and organic impurities is indispensable. From this follows the special design of our CF–IRMS application consisting of an injection port for a $\text{CO}_2/\text{N}_2\text{O}$ mixture, a flow-through tube cracker, a Nafion dryer, a cryofocus and a gas chromatograph (Fig. 2). Our system is linked to a MAT 253 via the open split of a conventional Precon GP-box system (Thermo Electron, Bremen). The components with their special features are described in detail in the following sections.

2.3.2 $\text{CO}_2/\text{N}_2\text{O}$ injection device

To fulfil the requirement of identical treatment of sample and reference within the cracker-GC-IRMS system (Fig. 2), a device was constructed allowing $\text{CO}_2/\text{N}_2\text{O}$ pulses to be injected into the cracker with a $10\ \mu\text{L}$ loop attached via the “SP1” six-port valve (Valco, USA). The CO_2 and N_2O concentration can be adjusted to appropriate values (~4% CO_2 in He, or ~8 nmol absolute per $10\ \mu\text{L}$ filling) by dilution of pure CO_2 and N_2O with He in a mixing chamber. With two pressure regulators (Porter 8286-SMVS-30, USA) the flow rate is set to $\sim 0.1\ \text{mL min}^{-1}$ for the $\text{CO}_2/\text{N}_2\text{O}$ mixture and $15\ \text{mL min}^{-1}$ for helium. This mixing device allows a convenient adjustment of the signal height of the CO_2 peaks without the need to switch between different loop sizes. To introduce a $\text{CO}_2/\text{N}_2\text{O}$ pulse, the SP1 valve is switched to the “inject” position and the GC flow ($0.85\ \text{mL min}^{-1}$) flushes the $\text{CO}_2/\text{N}_2\text{O}$ mixture from the $10\ \mu\text{l}$ loop via the “6P2” valve to the cracker device (Fig. 3).

2.3.3 Cracker

Alternatively to the $\text{CO}_2/\text{N}_2\text{O}$ pulses a sample can be introduced via the cracker device. The schematic layout of the cracker system can be seen in Fig. 3. The sealed tubes with the extracted CO_2 and N_2O are mounted into a flow-through tube cracker. After

A sublimation technique for high-precision measurements

J. Schmitt et al.

[Title Page](#)[Abstract](#)[Introduction](#)[Conclusions](#)[References](#)[Tables](#)[Figures](#)[◀](#)[▶](#)[Back](#)[Close](#)[Full Screen / Esc](#)[Printer-friendly Version](#)[Interactive Discussion](#)

flushing the cracker with helium, the tube is manually broken, its content is transferred out of the cracker passing a Nafion dryer and trapped on a cryofocus capillary. With an actuator the capillary is lifted out of the LN₂ to release the trapped gases, which are then directed to a GC column, where CO₂ is separated from N₂O and organic impurities before entering a continuous-flow isotope ratio mass spectrometer via an open split. A similar line for $\delta^{13}\text{C}$ determination at a precision of <0.05‰ was published earlier (Ferretti et al., 2000; Ribas-Carbo et al., 2002). The main difference is that a discrete amount of CO₂ (~20 nmol) enters our system via a special tube cracker device which allows us to achieve the same precision from only 2 mL STP compared to a total sample consumption of up to 45 mL from a large flask sample reservoir (Ferretti et al., 2000). To reduce the internal volume of the cracker to a minimum, the tube cracker is made of a 1/16–1/8" o.d. Swagelok reducing union, a 4.5 cm 1/8" o.d. stainless steel tubing, which is the flexible part and houses the glass tube, and a 1/8–1/16" o.d. Valco column end fitting. This fitting is equipped with a 2-µm stainless steel frit to prevent glass particles from the cracker entering the down stream part and potentially clogging the valve. The total internal volume of the cracker is only 160 µL, and the sample is flushed with a He flow rate of only 0.85 mL min⁻¹ to the cryofocus capillary.

2.3.4 Humidifier

High precision $\delta^{13}\text{C}$ measurements require low and constant water levels within the ion source since HCO₃⁺ production causes apparent sample enrichment (Leckrone and Hayes, 1998; Meier-Augenstein, 1999; Rice et al., 2001). Therefore, water vapour is generally kept at low levels within the carrier gas stream of CF-IRMS applications. Contrary to this common notion, a special humidifier device saturating the carrier gas with H₂O had to be inserted prior to the tube cracker device and consecutively the H₂O is removed again from the carrier via a Nafion dryer after passing the cracker. The reason for this unusual procedure was that although CO₂ pulses admitted to the cracker via the loop resulted in reproducible $\delta^{13}\text{C}$ values, similar measurements of CO₂ prepared in glass tubes revealed a serious fractionation with poor precision (>1‰).

A sublimation technique for high-precision measurements

J. Schmitt et al.

[Title Page](#)[Abstract](#)[Introduction](#)[Conclusions](#)[References](#)[Tables](#)[Figures](#)[◀](#)[▶](#)[◀](#)[▶](#)[Back](#)[Close](#)[Full Screen / Esc](#)[Printer-friendly Version](#)[Interactive Discussion](#)

2.3.5 Cryofocus, GC, IRMS injection

AMTD

4, 1853–1892, 2011

As cryofocusing capillary we use a loop of deactivated fused silica (0.32 mm o.d., 20 cm length) which can be immersed in LN₂ by a pneumatic actuator. The sharp sample pulse from the cryofocus is directed to the GC, where separation of CO₂ from N₂O and organic drilling contaminants is achieved at 110 °C using a GS-Carbonplot column (length 30 m, o.d. 0.32 mm, Agilent). A sample chromatogram shows that CO₂ is sufficiently separated from N₂O (Fig. 6a). An even better separation could be achieved using a lower GC temperature, however, this also results in a stronger separation of the CO₂ isotopologues, thus, increasing the time shift between *m/z* 44 and *m/z* 45 (Meier-Augenstein et al., 1996). Although this time shift can be accounted for by the software, we observed a stronger dependence of the isotopic ratio on the amount of the sample (usually referred to as linearity effects or amount dependency), a common phenomenon with GC-IRMS applications (Hall et al., 1999; Schmitt et al., 2003). Therefore, we choose a GC temperature of 110 °C, which results in a sufficient separation between CO₂ and N₂O of 14 s (see Fig. 6a) with still a moderate time shift of typically <0.1 s between the *m/z* 44 and *m/z* 45 beams. Nevertheless, we usually observe a small amount dependency of the measured $\delta^{13}\text{C}$ values, which has to be corrected for (see Sect. $\delta^{13}\text{C}$ correction).

Finally, the CO₂ and N₂O peaks pass the 2nd Nafion dryer and are transferred to a modified GP-Interface (Thermo Electron, Bremen, Germany) to be admitted to the ion source of the MAT 253 via the open split and inlet capillary with a flow rate of ~0.3 mL min⁻¹ STP.

Via the reference port and reference capillary (Fig. 3) we continuously introduce a small amount of carbon monoxide (~200 mV for *m/z* = 28 on the major cup with the standard resistor of $3 \times 10^8 \Omega$) to reduce adsorption-desorption effects of CO₂ at the surfaces of the ion source (Elsig and Leuenberger, 2010).

| | |
|--|------------------------------|
| Title Page | |
| Abstract | Introduction |
| Conclusions | References |
| Tables | Figures |
| ◀ | ▶ |
| ◀ | ▶ |
| Back | Close |
| Full Screen / Esc | |
| Printer-friendly Version | |
| Interactive Discussion | |

3.1 Sample preparation and sublimation extraction

Prior to the sublimation of an ice sample, each ice cube has to be prepared in the following way to provide a clean surface. With a band saw a cube is cut to the dimensions 3.5 cm \times 3.5 cm with 4.5 cm length. To fit this cube into the sublimation vessel with an internal diameter of 3.3 cm, the edges are rounded and trimmed with a stainless steel knife to a cylinder of \sim 3.2 cm diameter and a weight of \sim 30 g. The ice is inserted in the precooled sublimation vessel which is mounted to the flange via a copper gasket. First the atmospheric air is pumped out of the vessel until a constant value is reached corresponding to the vapour pressure of the ice. Since CO₂ adsorption on the surfaces is a critical issue, two hours at vacuum to decontaminate the system is necessary. As pointed out by others, CO₂ desorption from surfaces is most effective at high H₂O pressures (Zumbrunn et al., 1982; Güllük et al., 1998). With the cooling system, a temperature of \sim 34 °C is adjusted within the vessel leading to a pH₂O of \sim 0.25 mbar (pressure transducer “P_S” in Fig. 1). If the system is leak free, a final pressure of $<2 \times 10^{-7}$ mbar is achieved at the high vacuum side with bubble free ice and $\sim 5 \times 10^{-7}$ for bubble or clathrate ice due to slow sublimation of the ice, which releases some air. After two hours at vacuum, a few millimetres of ice have been removed and the surfaces of the vessel and the traps are sufficiently clean. The sublimation is started by increasing the current of the halogen bulbs and simultaneously decreasing the temperature of the cooling gas stream to -115 °C and adjusting its flow rate such that a pH₂O of \sim 0.25 mbar is obtained. Sampling is then started by cooling down the CO₂ trap and the air trap and opening V3. The gas stream liberated from the ice is now flowing towards the air trap. Collection of gas is stopped after 50 min by closing V3, V4 and V6 and cooling down the glass tube. After V5 is opened, the CO₂ trap is released from the LN₂ Dewar and warmed up for 60 s and CO₂ is transferred from the trap to the glass tube. Finally, the glass tube is flame sealed and stored until the GC-IRMS measurement. Parallel to the last steps, the air trap is removed from LN₂

[Title Page](#)

[Abstract](#)

[Introduction](#)

[Conclusions](#)

[References](#)

[Tables](#)

[Figures](#)

◀

▶

[Back](#)

[Close](#)

[Full Screen / Esc](#)

[Printer-friendly Version](#)

[Interactive Discussion](#)

as well and warmed to 100 °C. The air quantitatively desorbs from the molecular sieve and the constant pressure is read out at “ P_M ” (Fig. 1) to calculate the CO₂ and N₂O mixing ratios.

Note, that only ~85% of the ice sample is sublimated during the 50 min duration
5 leaving around 5 g of the ice sample in the vessel. A complete sublimation of the ice sample is not intended since ice impurities (mineral dust and organics) may gradually accumulate at the ice surface and could enhance chemical reactions when highly concentrated at the final stage. Additionally, the sublimation rate of the remaining ice piece is getting extremely slow. Regardless of this reasoning, leaving some ice unsublimated
10 does not compromise our 100% extraction efficiency, as the remaining ice stays entirely intact. This is different for conventional mechanic extractions, where initially the entire ice sample is crushed but the gas content is released only partially giving rise to fractionation of the measured mixing ratios (Lüthi et al., 2010).

3.2 Cracker-GC-IRMS measurement scheme

15 The high precision attainable using dual-inlet IRMS is based on the direct comparison of sample and reference of similar signal amplitude. Gas is admitted to the ion source by identically crimped capillaries. In contrast, for continuous flow applications, this identical treatment of sample and reference is accessible only to a certain degree, e.g. by using an internal reference inlet (Meier-Augenstein, 1997). The favoured
20 strategy is to bracket a sample peak with two references and try to adjust their signal heights as precisely as possible (Rice et al., 2001). For practical reasons, a precise adjustment is not completely possible, therefore the data has to be corrected using empirical functions for the amount dependency in $\delta^{13}\text{C}$ (see section data processing and correction functions). Our strategy outlined here is based on two different sets of
25 “referencing peaks”. Air standards admitted to the sublimation vessel during the sublimation of blank ice offer by far the closest analogue to gas samples extracted from ice. Due to large effort to produce them, it is unfeasible to use this type of reference for all correction purposes. But they are the basis on which the samples are referred to

[Title Page](#)[Abstract](#)[Introduction](#)[Conclusions](#)[References](#)[Tables](#)[Figures](#)[◀](#)[▶](#)[◀](#)[▶](#)[Back](#)[Close](#)[Full Screen / Esc](#)[Printer-friendly Version](#)[Interactive Discussion](#)

in terms of absolute value of $\delta^{13}\text{C}$ and the mixing ratios of CO_2 and N_2O . In contrast, $\text{CO}_2/\text{N}_2\text{O}$ injections automatically admitted to the cracker system with subsequent cryofocusing and GC separation face the same treatment as sample tubes and feature their identical peak shape. With these $\text{CO}_2/\text{N}_2\text{O}$ injections the system's $\delta^{13}\text{C}$ drift with

5 time and the dependence of $\delta^{13}\text{C}$ on the peak area ("linearity") are corrected for (see linearity section in Fig. 5). As pointed out above, identical measurement conditions are of paramount importance to attain a high precision $\delta^{13}\text{C}$ record from the samples. Therefore, we extract the air from several ice core samples and store the CO_2 in glass tubes until they are measured one after another in a single run. A typical measurement
10 session comprises up to 20 hours, starting with a "linearity section" consisting of pairs of an "equilibration peak" (EQ) followed by a "linearity peak". The size of the "linearity peak" is varied to produce three different peak heights (L3, L2 and L1), which can later be used to correct for amount effects. The injection of the $\text{CO}_2\text{--N}_2\text{O}$ mixture to the carrier gas stream is carried out by switching the valve "6P1", which injects $\sim 8\text{ nmol}$
15 CO_2 into the He stream. To produce linearity peaks with different peak sizes, the loop is filled and flushed out two or three times. A filling-injection cycle lasts for 3 s. Due to the cryofocus the peak shape for different sizes is identical for tube samples, which is a prerequisite for applying the identical treatment principle. The aim of preceding each "linearity peak" or sample peak with an equilibration peak (EQ) is to provide identical
20 conditions by equilibrating both the cracker-GC system and the ion source prior to all samples. This alternating EQ-L3, EQ-L2, EQ-L1 scheme is repeated five times until the actual sample tubes (SA) are measured (sample section in Fig. 5). Again, an equilibration peak precedes each sample tube, leading to an alternating EQ-SA scheme. As the process is fully automated except for the tube cracker itself, only the opening/closing of
25 the cracker and breaking the tube needs personal attendance.

To be loaded with a new sample tube, the cracker is opened and the glass shards of the last tube are removed. During that time the GC carrier flow (0.85 mL min^{-1}) bypasses the cracker via the "6P2" valve (Fig. 1), whereas the second He flow (cracker flow: 5 mL min^{-1}) sweeps the atmospheric air out to the vent after the cracker is closed.

A sublimation technique for high-precision measurements

J. Schmitt et al.

[Title Page](#)

[Abstract](#)

[Introduction](#)

[Conclusions](#)

[References](#)

[Tables](#)

[Figures](#)

◀

▶

[Back](#)

[Close](#)

[Full Screen / Esc](#)

[Printer-friendly Version](#)

[Interactive Discussion](#)

Flushing the cracker lasts for 60 s, the “6P2” valve is then switched back and the GC carrier flows through the cracker again. Before the sample tube is processed further, the preceding equilibration CO_2 peak is prepared by switching the “6P1” valve three times, injecting in total 8 nmol CO_2 from the $\text{CO}_2/\text{N}_2\text{O}$ mixture. The injected mixture 5 flows through the cracker to mimic the sample and then towards the cryofocus capillary immersed in LN2. After quantitative trapping (90 s) the capillary is lifted out of the LN2 and the sample directed to the GC where CO_2 is separated from N_2O . Via the open split, the CO_2 and N_2O peaks enter the ion source of the IRMS. After completion of the EQ peak, the sample tube is processed through bending the cracker, which breaks the 10 scored tube into two pieces releasing the stored gases into the GC carrier. All following steps are identical to the preparation of the EQ peak. Following this alternating EQ-SA scheme, all sample tubes are measured. A final “linearity section” completes the IRMS run to check whether the linearity of the system has changed during the measurement of the samples (not shown in Fig. 5).

15 4 Data processing and correction

4.1 Peak integration

To allow for a flexible and transparent peak integration, we use a self developed peak integration routine, similar to the software used by Bock et al. (2010). While the start 20 of the CO_2 peak is defined with a slope threshold criterion, the end of the CO_2 integral is determined using the first derivative of the m/z 44 beam (derivative decreases with the advent of the N_2O peak).

A special feature of our integration procedure is shown in Fig. 6b, which shows the 25 zoomed background region of the CO_2 peak. About 90 s before the CO_2 peak starts, the background drops by ca. 3 mV in case of m/z 44 beam. This step is due to the immersion of the cryofocus in LN2, which collects not only the current $\text{CO}_2/\text{N}_2\text{O}$ from the cracker for 90 s, but also a small fraction from the tail of the previous peak. To

| | |
|--|------------------------------|
| Title Page | |
| Abstract | Introduction |
| Conclusions | References |
| Tables | Figures |
| ◀ | ▶ |
| ◀ | ▶ |
| Back | Close |
| Full Screen / Esc | |
| Printer-friendly Version | |
| Interactive Discussion | |

account for this collected background, we calculate this “background area” and subtract this area from the proper peak area. Although this “background area” is small (~0.3 Vs compared to a m/z 44 area 120 Vs for a typical sample peak) and almost constant, correcting for it generally reduces the amount dependency of the $\delta^{13}\text{C}$ values, as this constant background area would otherwise add to a variable peak area.

To calculate the peak area for N_2O , only the beam m/z 44 is used, since we do not calculate isotope ratios. As the N_2O peak sits on the shoulder of the ca. 1000 fold larger CO_2 peak, the background correction is a critical step in determining the N_2O peak area. From the start of the N_2O peak backwards we take 10 s from the CO_2 tail and 5 s after the end of the N_2O peak. An exponential fit is calculated covering those background points before and after the N_2O peak. Using this fit, the N_2O peak is separated from the CO_2 peak and its area is integrated.

4.2 Referencing strategies and $\delta^{13}\text{C}$ corrections

Motivated by the identical treatment principle, we apply the following hierarchic referencing and correction strategy analogue to Behrens et al. (2008) to account for drift and fractionation processes throughout the entire system.

1. Pure CO_2 pulses of our monitoring gas are introduced by the reference port of the GP box at the beginning and at the end of a GC-IRMS measurement run (Fig. 5). These on/off pulses are used to monitor a drift in the isotope ratios or the beam intensity of the IRMS during the measurement run. These pulses cannot be used for any drift correction as they are admitted only at the start and end of the measurement, but they are helpful for troubleshooting and excluding errors in the IRMS source.
2. $\text{CO}_2/\text{N}_2\text{O}$ mixtures injected to the cracker system are used twofold. First, to correct for the temporal $\delta^{13}\text{C}$ drift caused by instability of the mass spectrometer itself, changing water levels, but also due to equilibration/saturation processes of

A sublimation technique for high-precision measurements

J. Schmitt et al.

[Title Page](#)

[Abstract](#)

[Introduction](#)

[Conclusions](#)

[References](#)

[Tables](#)

[Figures](#)

◀

▶

◀

▶

[Back](#)

[Close](#)

[Full Screen / Esc](#)

[Printer-friendly Version](#)

[Interactive Discussion](#)

the GC column occurring during the measurement time of >15 h (“drift correction”). Secondly, to provide the empirical relationship of the m/z 44 peak area to the $\delta^{13}\text{C}$ value (“linearity correction”), with which the amount dependency of the $\delta^{13}\text{C}$ values is corrected for.

5 3. Air reference samples processed with the sublimation extraction are the final reference basis for $\delta^{13}\text{C}$ and the mixing ratios of CO_2 and N_2O . Currently, we apply a “1-point calibration” using the results from the Boulder 2 cylinder, which is isotopically sufficiently close to our ice core samples. Within each GC-IRMS measurement run consisting of approximately 30 ice core samples, four to five of these air samples are randomly measured.

10

15 Therefore, the following data processing and correction scheme is applied on the raw $\delta^{13}\text{C}$ results of the peak integration routine. In a first step, the mean of the air reference samples is set to the assigned values of the cylinder. The next step is to correct for a $\delta^{13}\text{C}$ drift during the measurement run. Using all EQ peaks during the whole run, a cubic spline interpolation is performed and applied to all measured peaks types (EQ, L1–L3, and SA). Typically, the drift is on the order of $0.04\text{‰}\text{ h}^{-1}$. After this trend correction, the area- $\delta^{13}\text{C}$ relationship from three different peak sizes (L1, L2, L3) is calculated and all measured peaks are corrected for “linearity” effects (Hall et al., 1999; Schmitt et al., 2003). The typical slope of the area- $\delta^{13}\text{C}$ function is $0.002\text{‰}/\text{Vs}$. For ice core samples, ranging between 120 Vs for interglacial CO_2 values to 80 Vs for glacial values, this translates to a correction of 0.08‰ . After these corrections, the mean value of the air reference peaks is adjusted to the assigned value of the cylinder, thus, referencing all peaks of the measurement run with respect to Boulder 2.

20

A sublimation technique for high-precision measurements

J. Schmitt et al.

[Title Page](#)

[Abstract](#)

[Introduction](#)

[Conclusions](#)

[References](#)

[Tables](#)

[Figures](#)

◀

▶

[Back](#)

[Close](#)

[Full Screen / Esc](#)

[Printer-friendly Version](#)

[Interactive Discussion](#)

5.1 Measurement reproducibility

In the following, we discuss the measurement precision of the system, starting with the CO₂/N₂O pulses admitted to the cracker-GC-IRMS, followed by the air reference samples processed with the sublimation extraction and finally the ice core samples. The results are summarised in Table 1. As can be seen for the CO₂/N₂O injections, the precision for $\delta^{13}\text{C}$ depends on the peak size, with 1σ standard deviation of the small “L1” peaks 0.05‰ compared to 0.03‰ for the three times larger “L3” peaks. While for dual-inlet IRMS the measurement precision can be close to the theoretical shot noise limit (Merritt et al., 1995), for continuous flow-IRMS the precision is limited rather by the more complex sample preparation and the GC system. The precision of our air reference gases Boulder 1 and 2 is 0.05‰ and 0.04‰, thus, comparable to that of the CO₂/N₂O pulses. Therefore, the additional error from the gas processing in the sublimation extraction is small. During the last two years, several samples from different ice cores at different depth intervals were measured. These measurement precisions are compared in Table 1 as well. Overall, the precision ranges between 0.04‰ and 0.08‰, which is slightly lower than the precision for the reference gases. This is not surprising as additional effects can contribute to the variance of ice core samples. Notably chemical reactions of impurities within the ice core sample or during the sublimation, physical fractionation processes during the bubble close-off from the firm air and also processes during the drilling and storage of the ice core can alter the $\delta^{13}\text{C}$ composition. It is beyond the scope of this paper to discuss all these effects, nor does the current data basis yet allow firm conclusions, but there is indication that ice from the Talos Dome ice core is more reliable than from other cores. One hint for its “good ice quality” might be that its inorganic impurity content is much lower compared to the other ice cores, reducing the likelihood for chemical reactions and in-situ production of minute amounts of CO₂. This feature of the Talos Dome ice core can be observed

[Title Page](#)

[Abstract](#)

[Introduction](#)

[Conclusions](#)

[References](#)

[Tables](#)

[Figures](#)

◀

▶

◀

▶

[Back](#)

[Close](#)

[Full Screen / Esc](#)

[Printer-friendly Version](#)

[Interactive Discussion](#)

as well for new N_2O mixing ratio measurements recently obtained (Schilt et al., 2010), which showed no clear signs of in situ N_2O production as other ice cores.

As the mixing ratios for CO_2 and N_2O are calculated from both the total extracted air volume and the peak area of the mass spectrometric measurement, mixing ratios from $\text{CO}_2/\text{N}_2\text{O}$ pulses can not be derived. The precision for the mixing ratios for the air references and the ice cores are shown in Table 1. For CO_2 we obtain an average 1σ precision of ca. 1 ppmv for the air references and 2–3 ppmv for the different ice cores. This precision equals the precision of mechanic extraction techniques and other studies using the sublimation extraction (Güllük et al., 1998; Siegenthaler et al., 2005b; Lüthi et al., 2010). For N_2O we obtain a precision for reference air sample between 1.6 ppbv and 6.9 ppbv, and between 8.2 ppbv and 18.1 ppbv for the different ice cores. As pointed out above, most ice cores, but not Talos Dome, show problems with in situ N_2O production at certain age intervals. Therefore, the high scatter observed for EDML is at least in part due to the internal variability of the ice rather than an analytic problem. For the Talos Dome ice core we obtain a precision of 8–9 ppbv, which is a little less precise compared to the 5.6 ppbv achieved by other methods (Schilt et al., 2010).

If required, the precision for the mixing ratios can be improved further. As the primary focus of this new technique lies in high-precision $\delta^{13}\text{C}$ measurements, the devices and measurement procedure was optimised for $\delta^{13}\text{C}$, with the mixing ratios being 2nd priority. The main source of uncertainty in the mixing ratio results from flow changes in the cracker-GC-IRMS system, which translates into changes in peak size. This behaviour is visible in Fig. 5, where the amplitude of the “EQ” and “L3” peaks slightly increases between 200 min and 300 min. Although this does not affect the $\delta^{13}\text{C}$ values, it directly translates into the precision of the mixing ratios.

5.2 Comparison with previous ice core results

While determining the precision of a new method is relatively easy, it is more troublesome to quantify the accuracy. This is especially true for ice core analytics since

[Title Page](#)

[Abstract](#)

[Introduction](#)

[Conclusions](#)

[References](#)

[Tables](#)

[Figures](#)

◀

▶

◀

▶

[Back](#)

[Close](#)

[Full Screen / Esc](#)

[Printer-friendly Version](#)

[Interactive Discussion](#)

A sublimation technique for high-precision measurements

J. Schmitt et al.

[Title Page](#)[Abstract](#)[Introduction](#)[Conclusions](#)[References](#)[Tables](#)[Figures](#)[◀](#)[▶](#)[◀](#)[▶](#)[Back](#)[Close](#)[Full Screen / Esc](#)[Printer-friendly Version](#)[Interactive Discussion](#)

6 Conclusions

We have presented an analysis system capable of high precision measurements of $\delta^{13}\text{C}$ on CO_2 on ice core samples (1σ of 0.05%). Our system uses for the first time a sublimation technique, allowing a quantitative extraction for gases trapped in ice core samples. Additionally, the mixing ratios of CO_2 and N_2O can be derived with a precision of 2 ppmv and 8 ppbv, respectively, similar to conventional extraction systems. The various cold traps of the analysis system are equipped with cooling systems using liquid nitrogen regulated by controllers, allowing a highly automated system free of organic solvents.

The performance of the system was tested on a variety of Antarctic ice cores and different ice properties ranging from pure bubble ice, ice from the bubble/clathrate transition zone and pure clathrated ice proving the reliability and very high precision of our new method. With the 100% efficiency of our sublimation method we have now for the first time an extraction at hand that ensures unfractionated, high-precision $\delta^{13}\text{CO}_2$ analyses also in clathrated ice. This opens the window to the $\delta^{13}\text{CO}_2$ archive in central Antarctic ice from depths greater than about 700 m, where clathrate formation begins. For instance in the EPICA Dome C ice core these depths correspond to the time interval from 25 000 to 800 000 yr BP, i.e. the major part of the entire ice core record.

Acknowledgements. This work is a contribution to the European Project for Ice Coring in Antarctica (EPICA), a joint European Science Foundation/European Commission scientific programme, funded by the EU and by national contributions from Belgium, Denmark, France, Germany, Italy, the Netherlands, Norway, Sweden, Switzerland and the United Kingdom. The main logistic support was provided by IPEV and PNRA (at Dome C) and AWI (at Dronning Maud Land). Funding by the German Ministry of Education and Research (BMBF) through the German climate research program DEKLIM (project RESPIC) is acknowledged. The assistance of Melanie Behrens is gratefully acknowledged for running the MS and the organization of the labs. We also thank for the technical advice from Klaus-Uwe Richter.

[Title Page](#)

[Abstract](#)

[Introduction](#)

[Conclusions](#)

[References](#)

[Tables](#)

[Figures](#)

◀

▶

◀

▶

[Back](#)

[Close](#)

[Full Screen / Esc](#)

[Printer-friendly Version](#)

[Interactive Discussion](#)

5 Ahn, J. H., Brook, E. J., and Howell, K.: A high-precision method for measurement of paleoatmospheric CO₂ in small polar ice samples, *J. Glaciol.*, 55, 499–506, 2009.

Anklin, M., Barnola, J.-M., Schwander, J., Stauffer, B., and Raynaud, D.: Processes affecting the CO₂ concentrations measured in Greenland ice, *Tellus*, 47, 461–470, 1995.

10 Barnes, P. R. F., Wolff, E. W., Mallard, D. C., and Mader, H. M.: SEM Studies of the Morphology and Chemistry of Polar Ice, *Microsc. Res. Techniq.*, 62, 62–69, 2003.

Behrens, M., Schmitt, J., Richter, K.-U., Bock, M., Richter, U., Levin, I., and Fischer, H.: A gas chromatography/combustion/isotope ratio mass spectrometry system for high-precision $\delta^{13}\text{C}$ measurements of atmospheric methane extracted from ice core samples, *Rapid. Commun. Mass Spectrom.*, 22, 3261–3269, 2008.

15 Bock, M., Schmitt, J., Behrens, M., Möller, L., Schneider, R., Sapart, C., and Fischer, H.: A gas chromatography/pyrolysis/isotope ratio mass spectrometry system for high-precision δD measurements of atmospheric methane extracted from ice cores, *Rapid. Commun. Mass Spectrom.*, 24, 621–633, 2010.

Broecker, W. S. and Clark, E.: Holocene atmospheric CO₂ increase as viewed from the seafloor, *Global Biogeochem. Cy.*, 17, 1052, doi:10.1029/2002GB001985, 2003.

20 Brovkin, V., Hofmann, M., Bendtsen, J., and Ganopolski, A.: Ocean biology could control atmospheric $\delta^{13}\text{C}$ during glacial-interglacial cycle, *G-Cubed*, 3, 1–15, 2002.

Caldwell, W. E., Odom, J. D., and Williams, D. F.: Glass-Sample Tube Breaker, *Anal. Chem.*, 55, 1175–1176, 1983.

25 Des Marais, D. J. and Hayes, J. M.: Tube Cracker for Opening Glass-Sealed Ampoules under Vacuum, *Anal. Chem.*, 48, 1651–1652, 1976.

Elsig, J.: New insights into the global carbon cycle from measurements of CO₂ stable isotopes: methodological improvements and interpretation of a new EPICA Dome C ice core $\delta^{13}\text{C}$ record, Dissertation, University of Bern, 2009.

30 Elsig, J., Schmitt, J., Leuenberger, D., Schneider, R., Eyer, M., Leuenberger, M., Joos, F., Fischer, H., and Stocker, T. F.: Stable isotope constraints on Holocene carbon cycle changes from an Antarctic ice core, *Nature*, 461, 507–510, 2009.

Elsig, J. and Leuenberger, M. C.: C-13 and O-18 fractionation effects on open splits and on the ion source in continuous flow isotope ratio mass spectrometry, *Rapid. Commun. Mass Spectrom.*, 24, 1419–1430, doi:10.1002/rcm.4531, 2010.

A sublimation technique for high-precision measurements

J. Schmitt et al.

[Title Page](#)[Abstract](#)[Introduction](#)[Conclusions](#)[References](#)[Tables](#)[Figures](#)[◀](#)[▶](#)[◀](#)[▶](#)[Back](#)[Close](#)[Full Screen / Esc](#)[Printer-friendly Version](#)[Interactive Discussion](#)

A sublimation technique for high-precision measurements

J. Schmitt et al.

[Title Page](#)[Abstract](#)[Introduction](#)[Conclusions](#)[References](#)[Tables](#)[Figures](#)[◀](#)[▶](#)[Back](#)[Close](#)[Full Screen / Esc](#)[Printer-friendly Version](#)[Interactive Discussion](#)

Eyer, M.: Highly resolved $\delta^{13}\text{C}$ measurements on CO_2 in air from Antarctic ice cores, Dissertation, University of Bern, 2004.

Ferretti, D. F., Lowe, D. C., Martin, R. J., and Brailsford, G. W.: A new gas chromatograph-isotope ratio mass spectrometry technique for high-precision, N_2O -free analysis of $\delta^{13}\text{C}$ and $\delta^{18}\text{O}$ in atmospheric CO_2 from small air samples, *J. Geophys. Res.*, 105, 6709–6718, 2000.

Fischer, H., Wahlen, M., Smith, J., Mastroianni, D., and Deck, B.: Ice core records of atmospheric CO_2 around the last three glacial terminations, *Science*, 283, 1712–1714, 1999.

Fischer, H., Wahlen, M., and Smith, H. J.: Reconstruction of glacial/interglacial changes in the global carbon cycle from CO_2 and $\delta^{13}\text{CO}_2$ in Antarctic ice cores., *Memoirs of the National Institute for Polar Research*, 57, 121–138, 2003.

Frace, R. J., Allison, C. E., Etheridge, D. M., Trudinger, C. M., Enting, I. G., Leuenberger, M., Langenfelds, R. L., Michel, E., and Steele, L. P.: A 1000-year high precision record of $\delta^{13}\text{C}$ in atmospheric CO_2 , *Tellus*, 51B, 170–193, 1999.

Güllük, T., Slemr, F., and Stauffer, B.: Simultaneous measurement of CO_2 , CH_4 , and N_2O in air extracted by sublimation from Antarctica ice cores: Confirmation of the data obtained using other extraction techniques, *J. Geophys. Res.*, 103, 15971–15978, 1998.

Hall, J. A., Barth, J. A. C., and Kalin, R. M.: Routine Analysis by High Precision Gas Chromatography/Mass Selective Detector/Isotope Ratio Mass Spectrometry to 0.1 Parts Per Mil, *Rapid. Commun. Mass Spectrom.*, 13, 1231–1236, 1999.

Indermühle, A., Stocker, T. F., Joos, F., Fischer, H., Smith, H. J., Wahlen, M., Deck, B., Mastroianni, D., Tschumi, J., Blunier, T., Meyer, R., and Stauffer, B.: Holocene carbon-cycle dynamics based on CO_2 trapped in ice at Taylor Dome, Antarctica, *Nature*, 398, 121–126, 1999.

Kawamura, K., Nakazawa, T., Aoki, S., Sugawara, S., Fujii, Y., and Watanabe, O.: Atmospheric CO_2 variations over the last three glacial-interglacial climatic cycles deduced from the Dome Fuji deep ice core, Antarctica using a wet extraction technique, *Tellus B*, 55, 126–137, 2003.

Köhler, P. and Fischer, H.: Simulating changes in the terrestrial biosphere during the last glacial/interglacial transition, *Global Planet. Change*, 43, 33–55, 2004.

Leckrone, K. J. and Hayes, J. M.: Efficiency and Temperature Dependence of Water Removal by Membrane Dryers, *Anal. Chem.*, 69, 911–918, 1997.

Leckrone, K. J. and Hayes, J. M.: Water-Induced Errors in Continuous-Flow Carbon Isotope Ratio Mass Spectrometry, *Anal. Chem.*, 70, 2737–2744, 1998.

A sublimation technique for high-precision measurements

J. Schmitt et al.

[Title Page](#)[Abstract](#)[Introduction](#)[Conclusions](#)[References](#)[Tables](#)[Figures](#)[◀](#)[▶](#)[Back](#)[Close](#)[Full Screen / Esc](#)[Printer-friendly Version](#)[Interactive Discussion](#)

Leuenberger, M., Siegenthaler, U., and Langway, C. C.: Carbon isotope composition of atmospheric CO₂ during the last ice age from an Antarctic ice core, *Nature*, 357, 488–490, 1992.

Leuenberger, M. C., Eyer, M., Nyfeler, P., Stauffer, B., and Stocker, T. F.: High-resolution $\delta^{13}\text{C}$ measurement on ancient air extracted from less than 10 cm³ of ice, *Tellus*, 55B, 138–144, 2003.

Lourantou, A., Chappellaz, J., Barnola, J. M., Masson-Delmotte, V., and Raynaud, D.: Changes in atmospheric CO₂ and its carbon isotopic ratio during the penultimate deglaciation, *Quaternary Sci. Rev.*, 29, 1983–1992, 2010a.

10 Lourantou, A., Lavric, J. V., Köhler, P., Barnola, J. M., Paillard, D., Michel, E., Raynaud, D., and Chappellaz, J.: Constraint of the CO₂ rise by new atmospheric carbon isotopic measurements during the last deglaciation, *Global Biogeochem. Cy.*, 24, 1–15, 2010b.

Lüthi, D., Le Floch, M., Bereiter, B., Blunier, T., Barnola, J. M., Siegenthaler, U., Raynaud, D., Jouzel, J., Fischer, H., Kawamura, K., and Stocker, T. F.: High-resolution carbon dioxide concentration record 650 000–800 000 years before present, *Nature*, 453, 379–382, 2008.

15 Lüthi, D., Bereiter, B., Stauffer, B., Winkler, R., Schwander, J., Kindler, P., Leuenberger, M., Kipfstuhl, S., Capron, E., Landais, A., Fischer, H., and Stocker, T. F.: CO₂ and O₂/N₂ variations in and just below the bubble-clathrate transformation zone of Antarctic ice cores, *Earth Planet. Sc. Lett.*, 297, 226–233, 2010.

20 Meier-Augenstein, W., Watt, P., and Langhans, C.: Influence of Gas Chromatographic Parameters on Measurement of $^{13}\text{C}/^{12}\text{C}$ Isotope Ratios by Gas-Liquid Chromatography-Combustion Isotope Ratio Mass spectrometry, *J. Chromat. A*, 752, 233–241, 1996.

Meier-Augenstein, W.: A Reference Gas Inlet Module for Internal Isotopic Calibration in High Precision Gas-Chromatography, *Rapid. Commun. Mass Spectrom.*, 11, 1775–1780, 1997.

25 Meier-Augenstein, W.: Review: Applied gas chromatography coupled to isotope ratio mass spectrometry, *J. Chromat. A*, 842, 351–371, 1999.

Merritt, D. A., Freeman, K. H., Ricci, M. P., Studley, S. A., and Hayes, J. M.: Performance and Optimization of a Combustion Interface for Isotope Ratio Monitoring Gas Chromatography/Mass Spectrometry, *Anal. Chem.*, 67, 2461–2473, 1995.

30 Monnin, E., Indermühle, A., Dällenbach, A., Flückiger, J., Stauffer, B., Stocker, T. F., Raynaud, D., and Barnola, J.-M.: Atmospheric CO₂ concentration over the last termination, *Science*, 291, 112–114, 2001.

Petit, J. R., Jouzel, J., Raynaud, D., Barkov, N. I., Barnola, J.-M., Basile, I., Bender, M., Chap-

A sublimation technique for high-precision measurements

J. Schmitt et al.

[Title Page](#)

[Abstract](#)

[Introduction](#)

[Conclusions](#)

[References](#)

[Tables](#)

[Figures](#)

◀

▶

[Back](#)

[Close](#)

[Full Screen / Esc](#)

[Printer-friendly Version](#)

[Interactive Discussion](#)



pellaz, J., Davis, M., Delaygue, G., Delmotte, M., Kotlyakov, V. M., Legrand, M., Lipenkov, V. Y., Lorius, C., Pepin, L., Ritz, C., Saltzman, E., and Stievenard, M.: Climate and atmospheric history of the past 420 000 years from the Vostok ice core, Antarctica, *Nature*, 399, 429–436, 1999.

5 Ribas-Carbo, M., Still, C., and Berry, J.: Automated system for simultaneous analysis of ^{13}C , ^{18}O and CO_2 concentrations in small air samples, *Rapid. Commun. Mass Spectrom.*, 16, 339–345, 2002.

Rice, A. L., Gotoh, A. A., Ajie, H. O., and Tyler, S. C.: High-precision continuous-flow measurement of $\delta^{13}\text{C}$ and δD of atmospheric CH_4 , *Anal. Chem.*, 73, 4104–4110, 2001.

10 Schilt, A., Baumgartner, M., Schwander, J., Buiron, D., Capron, E., Chappellaz, J., Louergue, L., Schüpbach, S., Spahni, R., Fischer, H., and Stocker, T. F.: Atmospheric nitrous oxide during the last 140 000 years, *Earth Planet. Sc. Lett.*, 300, 33–43, doi:10.1016/j.epsl.2010.09.027, 2010.

Schmitt, J., Glaser, B., and Zech, W.: Amount-dependent isotopic fractionation during compound-specific isotope analysis, *Rapid. Commun. Mass Spectrom.*, 17, 970–977, 2003.

15 Schmitt, J.: A sublimation technique for high-precision $\delta^{13}\text{C}$ on CO_2 and CO_2 mixing ratio from air trapped in deep ice cores, Dissertation, University of Bremen, available at: <http://elib.suub.uni-bremen.de/diss/docs/00010568.pdf>, 2006.

Siegenthaler, U.: CO_2 -Konzentrationsmessungen an polaren Eisbohrkernen und Tests mit einer neuen Extraktionsmethode, Diplomarbeit, Bern, unpublished, 2002.

20 Siegenthaler, U., Monnin, E., Kawamura, K., Spahni, R., Schwander, J., Stauffer, B., Stocker, T. F., Barnola, J.-M., and Fischer, H.: Supporting evidence from the EPICA Dronning Maud Land ice core for atmospheric CO_2 changes during the past millennium, *Tellus*, 57, 51–57, 2005a.

25 Siegenthaler, U., Stocker, T. F., Monnin, E., Lüthi, D., Schwander, J., Stauffer, B., Raynaud, D., Barnola, J. M., Fischer, H., Masson-Delmotte, V., and Jouzel, J.: Atmospheric science: Stable carbon cycle-climate relationship during the late Pleistocene, *Science*, 310, 1313, doi:10.1126/science.1120130, 2005b.

Smith, H. J., Fischer, H., Wahlen, M., Mastroianni, D., and Deck, B.: Dual modes of the carbon cycle since the Last Glacial Maximum, *Nature*, 400, 248–250, 1999.

30 Werner, R. A. and Brand, W. A.: Referencing strategies and techniques in stable isotope ratio analysis, *Rapid. Commun. Mass Spectrom.*, 15, 501–519, 2001.

Wilson, A. T. and Long, A.: New approaches to CO_2 analysis in polar ice cores, *J. Geophys.*

Res., 102, 26601–26606, 1997.

Zhang, J., Quay, P. D., and Wilbur, D. O.: Carbon isotope fractionation during gas-water exchange and dissolution of CO_2 , *Geochim. Cosmochim. Ac.*, 59, 107–114, 1995.

Zumbrunn, R., Neftel, A., and Oeschger, H.: CO_2 measurements on 1- cm^3 ice samples with IR laserspectrometer (IRLS) combined with a new dry extraction device, *Earth Planet. Sc. Lett.*, 60, 318–324, 1982.

AMTD

4, 1853–1892, 2011

Discussion Paper | Discussion Paper

A sublimation technique for high-precision measurements

J. Schmitt et al.

[Title Page](#)

[Abstract](#)

[Introduction](#)

[Conclusions](#)

[References](#)

[Tables](#)

[Figures](#)

[◀](#)

[▶](#)

[◀](#)
[Back](#)

[▶](#)
[Close](#)

[Full Screen / Esc](#)

[Printer-friendly Version](#)

[Interactive Discussion](#)



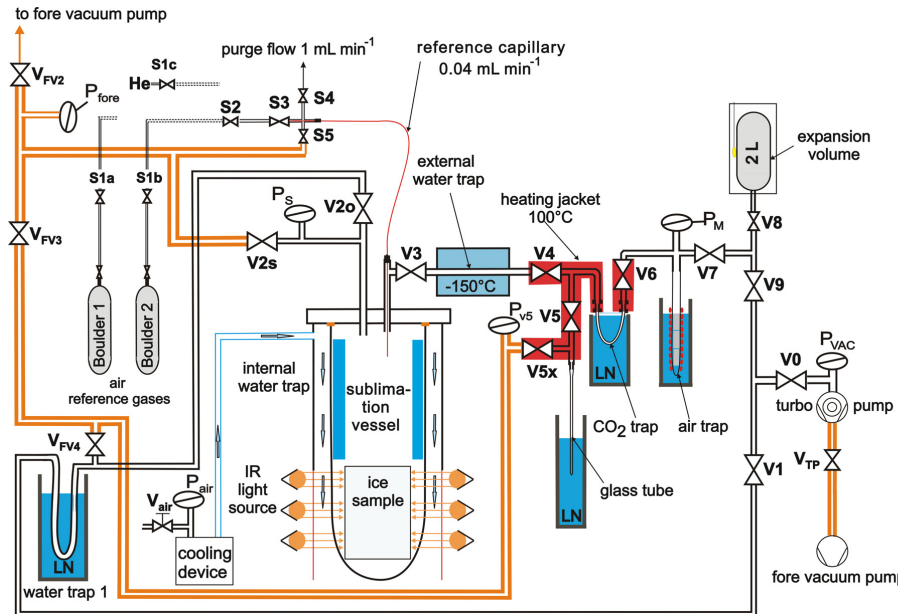
Table 1. The table shows the average reproducibility (1σ standard deviation) for measurements of calibrated air samples (Boulder 1 and 2 cylinders) and ice core samples for the parameters $\delta^{13}\text{C}$, and the mixing ratios of CO_2 and N_2O . Ice measurement were done on three different Antarctic ice cores, two EPICA drill sites (European Project for Ice Coring in Antarctica), EPICA-Dome C, or EDC, (at the Dome C drill site) and EPICA-DML (drill site at Dronning Maud Land), or EDML and the Talos Dome ice core, TALDICE. From these different cores, different depth ranges were analysed providing a range of physical and chemical ice properties. The column “ n ” denotes the number of replicates per sample. Column “ m ” denotes the total number of samples, where replicates have been measured.

| Type of measurement | CO_2 peak size (nmol) | n | m | $\delta^{13}\text{C}$ 1σ (%) | CO_2 1σ (ppmv) | N_2O 1σ (ppmv) |
|--|--------------------------------------|-----|------|--|-----------------------------------|--|
| $\text{CO}_2/\text{N}_2\text{O}$ pulses (L1) | 8 | 50 | 0.05 | – | – | – |
| $\text{CO}_2/\text{N}_2\text{O}$ pulses (L2) | 16 | 50 | 0.04 | – | – | – |
| $\text{CO}_2/\text{N}_2\text{O}$ pulses (L3) | 24 | 50 | 0.03 | – | – | – |
| “Boulder 1” CA06195 | 16 | 4 | 3 | 0.050 | 0.9 | 1.6 |
| “Boulder 2” CA06818 | 26 | 4 | 12 | 0.037 | 1.3 | 6.9 |
| bubble ice EDC (100 m–600 m) | 16–24 | 3 | 28 | 0.061 | 1.9 | 8.6 |
| clathrate ice EDC (>1200 m) | 16–24 | 3 | 27 | 0.082 | 2.6 | 9.9 |
| mixing zone Talos (600 m–1200 m) | 16–20 | 3 | 4 | 0.036 | 1.5 | 8.9 |
| clathrate ice Talos (>1200 m) | 18–24 | 3 | 15 | 0.048 | 2.6 | 8.2 |
| clathrate ice EDML (>1200 m) | 18–24 | 3 | 8 | 0.053 | 1.8 | 18.1 |

- [Title Page](#)
- [Abstract](#) [Introduction](#)
- [Conclusions](#) [References](#)
- [Tables](#) [Figures](#)
- [◀](#) [▶](#)
- [◀](#) [▶](#)
- [Back](#) [Close](#)
- [Full Screen / Esc](#)
- [Printer-friendly Version](#)
- [Interactive Discussion](#)

A sublimation technique for high-precision measurements

J. Schmitt et al.



A sublimation technique for high-precision measurements

J. Schmitt et al.

Title Page

Abstract

Conclusions | References

Tables | Figures

◀ ▶

◀

[Back](#)

Full Screen / Esc

[Printer-friendly Version](#)

Interactive Discussion



Fig. 2. Photo showing the sublimation vessel with a loaded ice sample and the infrared source. The cooling jacket starts just above the ice sample and a cold air stream is fed in from both sides. The infrared source consists of 18 bulbs mounted on a holder, and the red foil visible in the central part. During the sublimation of the ice sample the infrared source is moved upwards, hence the section with sample is surrounded by the bulbs.

A sublimation technique for high-precision measurements

J. Schmitt et al.

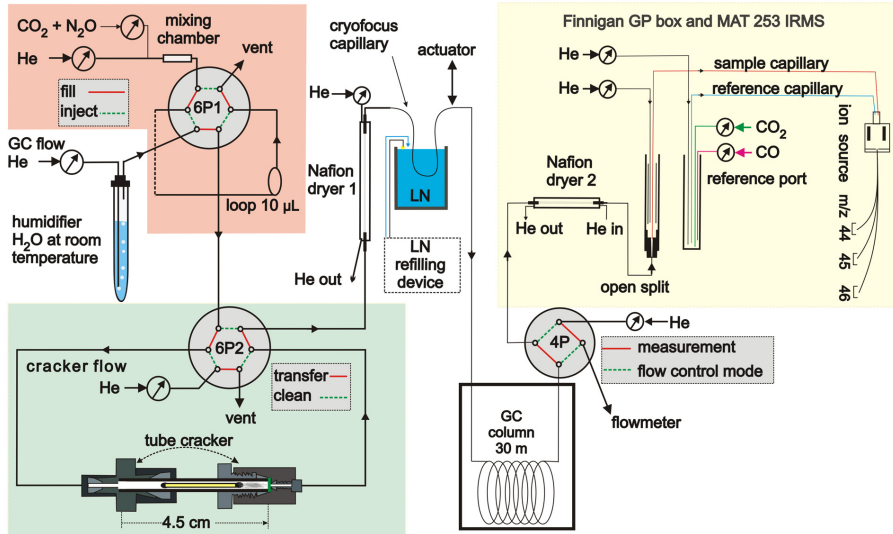
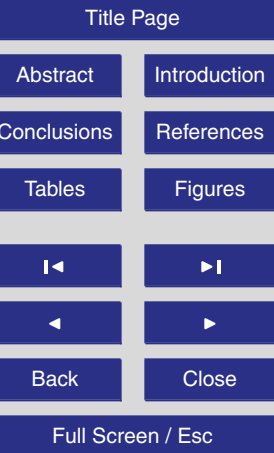


Fig. 3. Flow scheme of the tube cracker-GC-IRMS line with a device to introduce $\text{CO}_2/\text{N}_2\text{O}$ pulses into the GC carrier gas (red box), the tube cracker (green box), followed by a Nafion dryer, cryofocus capillary, GC, 2nd Nafion dryer and finally the inlet system with the open split leading to the ion source of the IRMS and the reference port to inject CO_2 std/on off peaks and to admit a continuous CO background (yellow box).



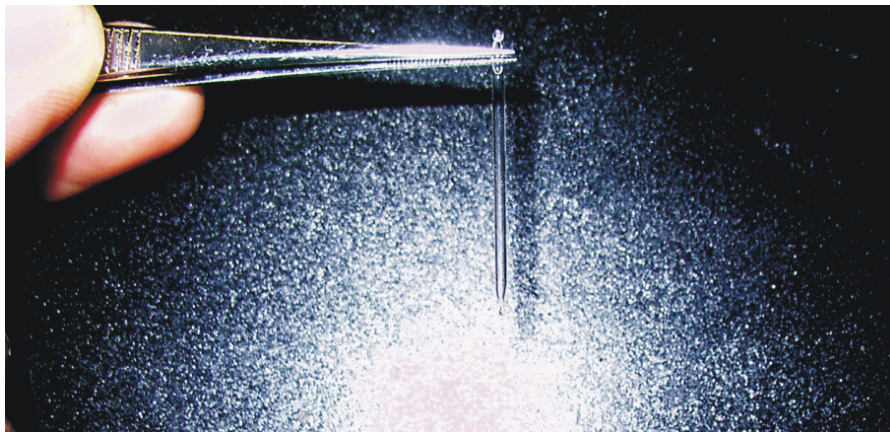


Fig. 4. Photo showing the closed sample tube.

A sublimation technique for high-precision measurements

J. Schmitt et al.

[Title Page](#)

[Abstract](#)

[Introduction](#)

[Conclusions](#)

[References](#)

[Tables](#)

[Figures](#)

◀

▶

◀

▶

[Back](#)

[Close](#)

[Full Screen / Esc](#)

[Printer-friendly Version](#)

[Interactive Discussion](#)

A sublimation technique for high-precision measurements

J. Schmitt et al.

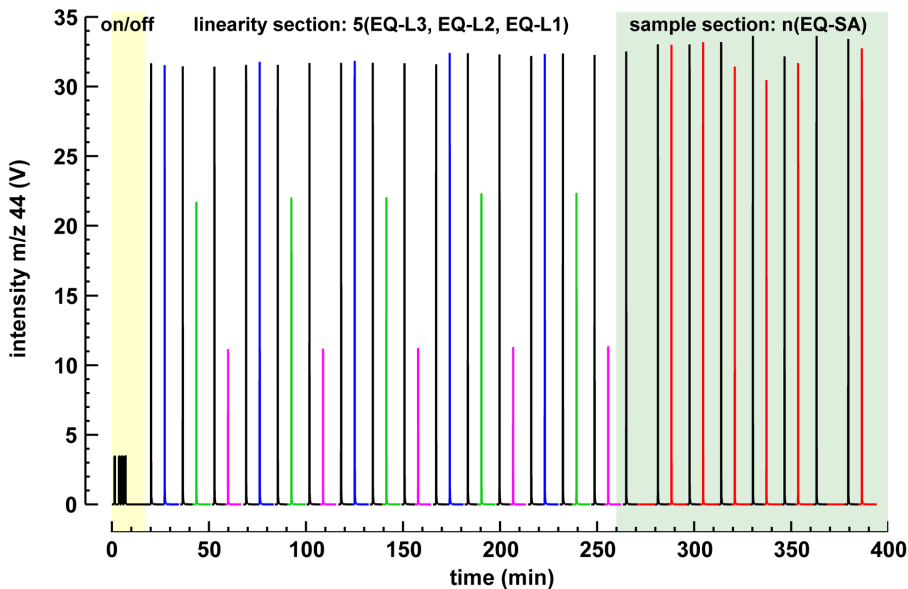


Fig. 5. Chromatogram showing the first 400 min of a typical measurement session comprising up to 1500 min. Within the first 10 min pure CO₂ pulses are introduced by the reference port of GP box (so called std on/off peaks). The “linearity section” runs from 15 min to 260 min, where pulses of a CO₂/N₂O mixture are introduced into the tube cracker GC system. The “linearity peaks” are produced in three size classes, L3 in blue, L2 in green, L1 in magenta; each “linearity peak” is preceded by an “equilibrium peak”, EQ in black. This scheme of EQ-L3, EQ-L2, EQ-L1 (= one block) is then repeated five times. In the following “sample section”, starting at 260 min, the first eight measured sample tubes are shown (in red), with the sample 1 and sample 7 being empty tubes. Identical measurement conditions for each of these peaks are provided by an equilibration peak (EQ in black) preceding each of them. After all sample tubes have been processed, a second “linearity section”, consisting of four blocks, followed by a series of std on/off closes the measurement session (not shown).

Title Page

Abstract

Introduction

Conclusion

References

Tables

Figures

1

1

◀

Back

Close

Full Screen / Esc

[Printer-friendly Version](#)

Interactive Discussion

A sublimation technique for high-precision measurements

J. Schmitt et al.

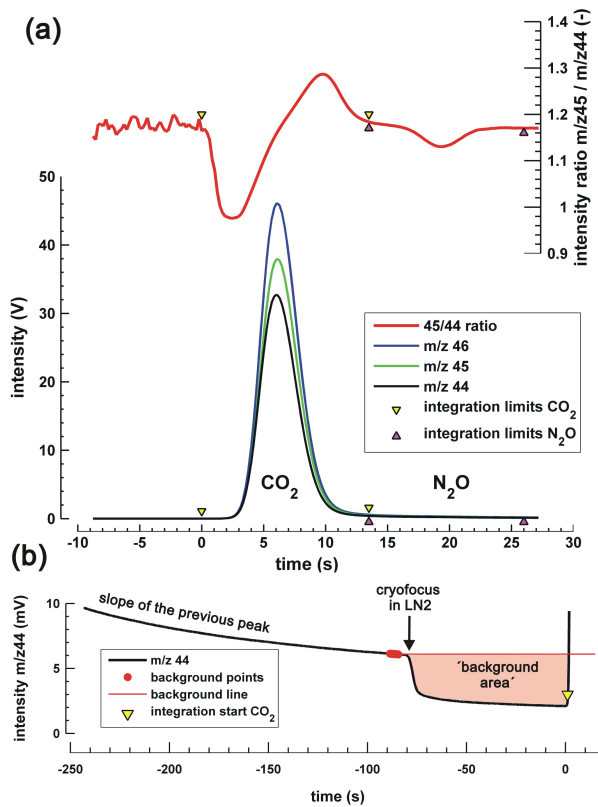


Fig. 6. (a) Chromatogram showing the separation of CO_2 from N_2O for an ice core sample. The N_2O peak is clearly visible in the measured m/z 45/44 beam ratio as a negative bump since the average molecular mass of N_2O is lower than that of CO_2 . However, as the typical atmospheric abundance of N_2O is only 1/1000 of CO_2 , the N_2O peak is not visible in the intensity plot below. **(b)** Zoom into the region prior to the CO_2 peak start to illustrate the background in front of the peak. The background is determined around 85 s before the peak start.

Title Page

Abstract

Introduction

Conclusions

References

Tables

Figures

1

Bac

Close

Full Screen / Esc

Printer-friendly Version

Interactive Discussion

A sublimation technique for high-precision measurements

J. Schmitt et al.

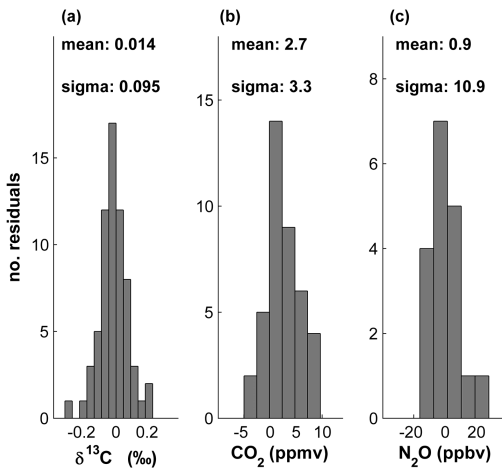


Fig. 7. **(a)** Comparison of $\delta^{13}\text{C}$ results obtained with the sublimation technique with results using a mechanic cracker device on the same ice core (Elsig et al., 2009). Shown are the differences between the sublimation and the cracker results measured on the EDC ice core over the depth interval from 110 m to 580 m (pure bubble ice). Differences were calculated where both methods measured neighbouring ice samples, which have air occluded which can be regarded identical for this purpose (mean age differences <25 years), when taking the averaging effect of the bubble enclosure process into account. **(b)** Comparison of CO_2 concentration measurements obtained with our sublimation extraction with published data from the same ice core using a mechanic extraction device (Monnin et al., 2001). Within the covered depth range the entrapped ice core air exists only within bubbles (“bubble ice”). The measured depth interval covers the time interval of the last deglaciation, thus, covers CO_2 concentrations between 185 and 265 ppm, i.e. almost the full range of the glacial/interglacial CO_2 variability. **(c):** comparison of N_2O concentration measurements obtained with our sublimation extraction with published data from the same ice core using a melt extraction device (Schilt et al., 2010). At this depth range, the bubbles have transformed into clathrate hydrates (“clathrate ice”). The selected time interval (65–90 ka) includes rapid N_2O variations between 210 and 265 ppmv, thus, covers almost the full natural variability during the last 800 ka.

[Title Page](#)

[Abstract](#)

[Introduction](#)

[Conclusions](#)

[References](#)

[Tables](#)

[Figures](#)

[◀](#)

[▶](#)

[◀](#)

[▶](#)

[Back](#)

[Close](#)

[Full Screen / Esc](#)

[Printer-friendly Version](#)

[Interactive Discussion](#)